

Can Targeted Clean-Label Poisoning Attacks Generalize?

Zhizhen Chen¹ Subrat Kishore Dutta^{2,3}
Zhengyu Zhao¹ Chenhao Lin¹ Chao Shen¹ Xiao Zhang³
¹Xi'an Jiaotong University ²Saarland University
³CISPA Helmholtz Center for Information Security

zhizhenc@stu.xjtu.edu.cn {subrat.dutta, xiao.zhang}@cispa.de
{zhengyu.zhao, linchenhao}@xjtu.edu.cn chaoshen@mail.xjtu.edu.cn

Abstract

Targeted poisoning attacks aim to compromise the model's prediction on specific target samples. In a common clean-label setting, they are achieved by slightly perturbing a subset of training samples given access to those specific targets. Despite continuous efforts, it remains unexplored whether such attacks can generalize to unknown variations of those targets. In this paper, we take the first step to systematically study this generalization problem. Observing that the widely adopted, cosine similarity-based attack exhibits limited generalizability, we propose a well-generalizable attack that leverages both the direction and magnitude of model gradients. In particular, we explore diverse target variations, such as an object with varied viewpoints and an animal species with distinct appearances. Extensive experiments across various generalization scenarios demonstrate that our method consistently achieves the best attack effectiveness. For example, our method outperforms the cosine similarity-based attack by 20.95% in attack success rate with similar overall accuracy, averaged over four models on two image benchmark datasets. The code is available at https://github.com/jiaangk/generalizable_tcpa.

1. Introduction

Training modern machine learning models often requires a vast amount of data, which is often crawled from the internet [6, 11, 34, 37]. However, the data published by untrusted third parties may be collected as part of the training set [5], where a malicious adversary can leverage this to disrupt the model's behavior [4, 15, 21, 28, 43, 46]. Such a security threat, regarded as one of the biggest concerns in the machine learning industry [22], is known as data poisoning attacks, corrupting models in inference time with a modified training set. According to Cinà et al. [7], data poisoning attacks can be roughly divided into three categories: indis-

criminate, targeted, and backdoor poisoning attacks. Indiscriminate poisoning attacks corrupt the victim model, maximizing the model's test error in inference time [9, 10, 18]. Backdoor poisoning attacks create a backdoor in the victim model, altering the model's output when the input is a triggered sample [24, 33, 38]. This paper focuses on targeted poisoning attacks, where the adversarial goal is to compromise the model's behavior on specific inputs [1, 12, 19]. Targeted poisoning attacks are stealthier than indiscriminate poisoning attacks since they have negligible impact on the model's overall accuracy and do not require any input modifications during inference time like backdoor attacks.

Earlier works on data poisoning consider noisy-label attacks, where the adversary directly inserts samples with wrong labels into the training set [3, 4, 43–45]. However, such attacks can not be realized if the adversary does not have control of the labeling process, and a human examiner might easily spot the noisy-label poisons. Recent works focus on developing clean-label poisoning attacks [9, 33, 36], where the adversary aims to poison the training set with carefully crafted but imperceptible noises. The poisoned samples look visually indistinguishable from their clean counterparts, enabling these attacks to be effective even in the presence of a human observer who scrutinizes the whole training dataset. Although clean-label poisoning attacks have been extensively studied [12, 19, 36], existing works are often limited to the ideal scenario where the target samples are known to the adversary and used during optimization. However, in practical scenarios, the adversary may not have precise knowledge of the target since the actual target may exhibit large variations from the samples used to optimize the adversary. For example, when an adversary plans to compromise an autonomous driving system's recognition of a stop sign, they should consider the potential variations of the sign regarding distance, angle, background, etc.

To address the above limitation of existing work, in this paper, we study the generalizability of targeted clean-label poisoning attacks to unknown variations of targets. Figure 1

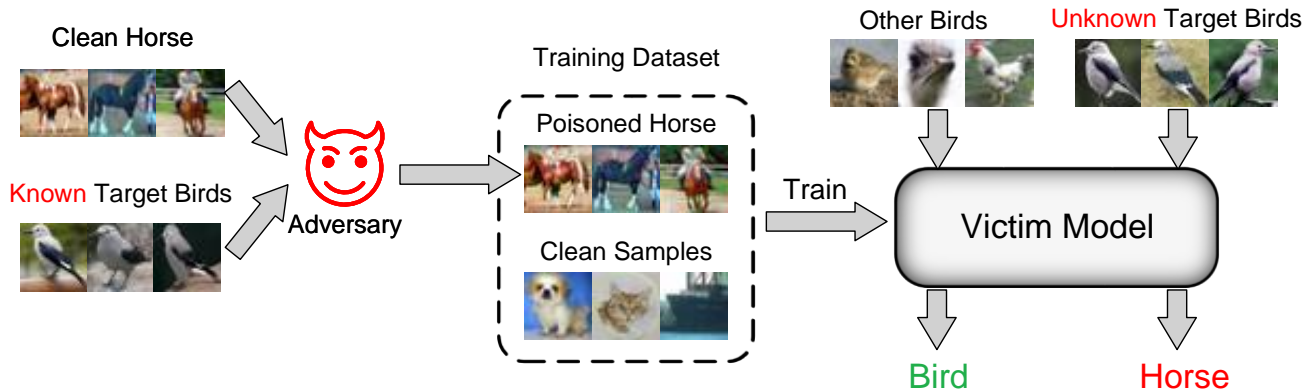


Figure 1: The schematic of our proposed poisoning attack. The adversary poisons training samples towards known (clean) targets in a clean-label manner, i.e., by slightly perturbing images. When the victim retrains the model, the poisoning effects generalize to unknown (clean) targets that fall into the same subpopulation as the known targets, with little impact on other (clean) samples.

illustrates the overall attack pipeline. Specifically, we form the variations of a target as a subpopulation distribution, inspired by the literature on (noisy-label) subpopulation attacks [17, 20]. We explore two types of variations representing varying difficulties of generalization, from an object with varied viewpoints (Multi-View Car) to an animal species with varied appearances (CUB-200-2011).

We observe that the widely adopted, cosine similarity-based attack method, *Witches' Brew* [12], does not generalize well. To address this issue, we analyze its mechanism and propose to incorporate the Euclidean distance, leading to a new attack method that leverages both the gradient direction and magnitude. Extensive experiments across various generalization scenarios, including different targets, model architectures, datasets, and training paradigms, demonstrate that our method consistently achieves the best attack effectiveness. For example, our method outperforms *Witches' Brew* by 20.95% in attack success rate with comparable overall accuracy, averaged over four models on two datasets. We make the following main contributions:

- Our work, for the first time, explores the generalizability of targeted clean-label poisoning attacks, where the adversary aims to generalize the poisoning effects from specific samples of the target used for the attack optimization to its unknown variations.
- We propose a simple yet effective attack method, which leverages both the gradient direction and magnitude for optimization, largely surpassing existing methods in generalizability and also securing the new state-of-the-art performance on the conventional benchmark.
- We further demonstrate the superiority of our method in other generalization aspects, such as cross-model-architecture and cross-training-setup.

2. Related Work

Data poisoning attacks pose threats to the availability and integrity of a machine learning system [7, 13]. We focus on integrity poisoning attacks that target only specific clean samples, in contrast to availability poisoning attacks [3, 4, 9, 10, 18], which induce indiscriminate prediction errors.

Targeted Data Poisoning Attacks. Targeted poisoning attacks are training-only attacks [13] that do not modify the sample in inference time. For example, Koh and Liang [21] introduced the targeted poisoning attack that manipulates the model to misclassify the specific samples to the wrong class. Muñoz-González et al. [28] formulated the targeted poisoning attack into a bi-level optimization problem. Later, Shafahi et al. [36] proposed clean-label poisoning attacks that attack specific test instances without label tampering in the linear transfer learning scenario. Zhu et al. [47] constructed poison samples that form a convex polytope around the target sample, increasing the probability that the target falls within the attack zone in the feature space, and Aghakhani et al. [1] further developed this idea. Huang et al. [19] introduced *MetaPoison*, a clean-label data poisoning method that solves the bi-level optimization problem to craft poisons capable of fooling deep neural networks, even when trained from scratch. More recently, Geiping et al. [12] introduced *Witches' Brew*, which employs gradient matching to craft poisons, achieving a higher attack success rate in the training-from-scratch scenario and reducing the time of the adversarial process. Our work follows these conventional studies but extends their scope regarding the target. Specifically, instead of considering target samples that are known during attack optimization, we consider a more realistic scenario in which the adversary targets the

variations of their known samples.

Backdoor Attacks. Backdoor attacks consider generalization across samples, but they are not training-only attacks since they also modify testing samples (at the inference time) by injecting triggers. Gu et al. [16] first introduced the backdoor attacks, where models behave normally on clean inputs but misclassify specific inputs with backdoor triggers. Several works focus on constructing imperceptible triggers. However, these methods either require controlling the training process [8, 23, 29] or injecting a large number of poison samples into the training set [2, 24, 25]. The first attempt to leverage adversarial samples to implement backdoor poisoning attacks is [33], which employed a feature collision approach similar to [36]. Souri et al. [38] focused on the training-from-scratch scenario that leveraged the gradient alignment attack method with several practical techniques (data selection, model retraining), successfully conducting the attack with a smaller budget (1% size of the training set). Some backdoor attacks have been investigated using natural objects as the backdoor trigger [41, 42], but such object triggers do not act as variations of the target as in our studied problem.

Subpopulation Poisoning Attacks. Subpopulation poisoning attacks also aim to compromise the model performance on a subpopulation, which is proposed by Jagielski et al. [20]. Rose et al. [32] and Gupta et al. [17] have further explored the subpopulation’s susceptibility in different model architectures. However, these studies only performed noisy-label attacks with label flipping, and the size of the poisoned subpopulation is not usually small. Sometimes, the size can even exceed 10% of the training set [17], which inevitably affects the model’s overall accuracy. Differently, our attack considers the clean-label manner, following the targeted poisoning attack’s threat model. In addition, it only modifies a small subset (typically 1%) of training data, aiming at little impact on the model’s overall accuracy.

3. Preliminary

In this section, we introduce the necessary notations for understanding the threat model and the general procedure for creating targeted clean-label poisoning samples.

Specifically, we refer to a model with parameter θ as $F(\cdot, \theta)$. A sample can be described as (\mathbf{x}, y) where $\mathbf{x} \in \mathbb{R}^n$ is the instance and y is the corresponding label. When the model takes \mathbf{x} as input, the output of the model is $F(\mathbf{x}, \theta)$. A dataset is a set of samples that $\mathcal{S} = \{(\mathbf{x}_i, y_i)\}_{i=1}^N$. We assume that all the instances \mathbf{x} in \mathcal{S} are i.i.d. sampled from the underlying data distribution \mathcal{D} . The training process of a classification model can be simplified to minimize average loss over the training set. More formally, the model by

solving the following optimization problem:

$$\min_{\theta} \frac{1}{N} \sum_{i=1}^N \ell(F(\mathbf{x}_i, \theta), y_i),$$

where ℓ stands for the individual loss function, such as cross-entropy loss, defined with respect to (\mathbf{x}_i, y_i) and θ .

Targeted Poisoning Attacks. We formulate the targeted poisoning attack as a security game between an adversary and a victim model trainer following prior work [7, 39]:

1. The adversary has the knowledge of the model’s training dataset \mathcal{S} and target samples $\{\mathbf{x}_i^t\}_{i=1}^T$;
2. The adversary’s knowledge and capability depends on whether the attack setting is *white-box* or *black-box*;
3. The adversary generates a poisoned training set \mathcal{S}' by poisoning a subset (usually less than 1%) of \mathcal{S} ;
4. The victim model trainer employs the poisoned set \mathcal{S}' to train a poisoned model with parameters θ' .

The goal of the adversary is to make the model $F(\cdot, \theta')$ misclassify any target sample in $\{\mathbf{x}_i^t\}_{i=1}^T$ to some intended class y^{adv} without compromising its overall accuracy, i.e., the classification accuracy on the data distribution \mathcal{D} . The *white-box* setting often discussed in recent work is that the adversary knows the architecture of the victim model F . The adversary does not know the victim’s model in *black-box* setting. This paper mainly focuses on the poisoning attack in the *white-box* setting. We also demonstrated that our attack method remains effective in the *black-box* setting.

Clean-label poisoning attacks alter the source samples by adding imperceptible perturbations, which are harder to detect than label flipping in noisy-label attacks. Following previous works [1, 12, 33, 38], we consider L_∞ -norm bounded perturbations as the clean-label poisoning setting in this work. For the ease of presentation, we separate the whole training set \mathcal{S} into a clean set \mathcal{S}_c (that will not be poisoned) and the remaining set \mathcal{S}_p (that will be poisoned):

$$\mathcal{S} = \mathcal{S}_p \cup \mathcal{S}_c, \quad \mathcal{S}_p \cap \mathcal{S}_c = \phi, \quad \mathcal{S}_p = \{(\mathbf{x}_i^p, y_i^p)\}_{i=1}^P.$$

The adversary is allowed to inject imperceptible perturbations to the small training subset \mathcal{S}_p to obtain the poisoned set \mathcal{S}'_p . Let \mathcal{C} be the collection of feasible sets of P poisoning perturbations, which captures the attack constraints:

$$\mathcal{C} = \{(\boldsymbol{\delta}_1, \boldsymbol{\delta}_2, \dots, \boldsymbol{\delta}_P) : \boldsymbol{\delta}_i \in \mathbb{R}^n, \|\boldsymbol{\delta}_i\|_\infty \leq \varepsilon, \forall i \in [P]\}. \quad (1)$$

Here, the ε -bound in L_∞ -norm ensures that the injected perturbations remain imperceptible and the poisoned samples have clean labels. For any $\Delta = (\boldsymbol{\delta}_1, \boldsymbol{\delta}_2, \dots, \boldsymbol{\delta}_P) \in \mathcal{C}$, the poisoned training set is given by:

$$\mathcal{S}'(\Delta) = \mathcal{S}'_p(\Delta) \cup \mathcal{S}_c, \quad \mathcal{S}'_p(\Delta) = \{(\mathbf{x}_i^p + \boldsymbol{\delta}_i, y_i^p)\}_{i=1}^P. \quad (2)$$

Denote by \mathcal{L} the averaged training loss with the option of employing some data augmentation techniques:

$$\mathcal{L}(F, \mathcal{A}, \theta, \mathcal{S}) = \frac{1}{|\mathcal{S}|} \sum_{(\mathbf{x}, y) \in \mathcal{S}} \ell(F(\mathcal{A}(\mathbf{x}), \theta), y),$$

where \mathcal{A} is the data augmentation the victim may apply to the training samples. Then, the objective of targeted clean-label poisoning attacks can be mathematically defined as the following bi-level optimization problem [12, 19, 28]:

$$\begin{aligned} \Delta^* = \arg \min_{\Delta \in \mathcal{C}} \sum_{i=1}^T \ell(F(\mathbf{x}_i^t, \theta'), y^{\text{adv}}), \\ \text{s.t. } \theta' = \arg \min_{\theta} \mathcal{L}(F, \mathcal{A}, \theta, \mathcal{S}'(\Delta)), \end{aligned} \quad (3)$$

where $\Delta \in \mathcal{C}$ is a feasible set of P poisoning perturbations defined by Equation 1, and $\mathcal{S}'(\Delta)$ is the corresponding poisoned training dataset defined by Equation 2. In the following discussions, when Δ is free of context, we write $\mathcal{S}' = \mathcal{S}'(\Delta)$ and $\mathcal{S}'_p = \mathcal{S}'_p(\Delta)$ for simplicity.

4. Generalizable Targeted Poisoning Attacks

In this section, we first introduce our threat model, which follows the above setup of clean-label targeted poisoning attacks but differs in the target, i.e., our target samples are *not known* to the adversary during their optimization. Then, we describe the technical details of our proposed attack method, which is effective not only in our threat model but also in the conventional threat model.

4.1. Threat Model

We assume that the target samples follow a certain distribution \mathcal{D}_t . The adversary in our threat model does not know the exact target samples during optimization. Instead, the adversary can only optimize their attack based on T samples following \mathcal{D}_t , and they expect the poisoning effects to generalize to unknown samples from the same \mathcal{D}_t . This threat model enables the adversary to compromise a group of homogeneous samples (e.g., a specific type of stop sign mentioned earlier), which is more realistic than the conventional threat model, which targets the identical known sample(s). By adopting the bi-level optimization in Equation 3 for our threat model, we obtain:

$$\begin{aligned} \Delta^* = \arg \min_{\Delta \in \mathcal{C}} \mathbb{E}_{\mathbf{x} \sim \mathcal{D}_t} [\ell(F(\mathbf{x}, \theta'), y^{\text{adv}})] \\ \text{s.t. } \theta' = \arg \min_{\theta} \mathcal{L}(F, \mathcal{A}, \theta, \mathcal{S}'(\Delta)), \end{aligned} \quad (4)$$

where the specific target samples in conventional targeted poisoning attacks become a certain distribution \mathcal{D}_t . Note that different from subpopulation attacks [17, 20, 32], we consider the subpopulation to be small such that the model’s overall accuracy would not be affected too much.

4.2. Our Attack Framework

Previous targeted poisoning attacks were optimized based on a single target. When we directly perform the targeted poisoning attack, *Witches’ Brew* [12], in our threat model, the attack success rate to a bird species is 39.06% (see Table 1 in Section 5.1 for more details). To address this limitation, we propose our attack framework with a set of targets in Algorithm 1, offering a practical framework for generalizable targeted clean-label poisoning attacks.

Our framework is inspired by the successful practice in backdoor attacks [15], where directly inserting noisy-label triggers towards a target distribution with the intended class y^{adv} is effective in compromising the classification. However, in our clean-label setting, we cannot directly add noisy-label samples (and we do not apply triggers). Instead, we optimize the perturbations Δ to make the poisoned set \mathcal{S}'_p “similar” to target samples from \mathcal{D}_t to the most extent.

Retraining Step. We introduce the retraining step into our framework. This technique is first introduced by Souri et al. [38], where they apply this to the hidden-trigger backdoor poisoning attack. When the model retrains on the dataset with the perturbations during the adversarial process, it will dynamically reflect the effect of the current perturbation. Our ablation study in Section 5.2 demonstrates this technique can also play a role in the subpopulation target attack.

Multi-Targeted Adversarial Loss. Let $D(\mathcal{S}'_p, \mathcal{S}_t)$ denote the adversarial loss between \mathcal{S}'_p and \mathcal{S}_t in a certain surrogate model $F(\cdot, \theta)$, where \mathcal{S}_t denotes a set of target data points i.i.d. sampled from \mathcal{D}_t . The adversary aims to minimize $D(\mathcal{S}'_p, \mathcal{S}_t)$ to make the poisoned set play a similar role to the target set in the training process. Different attack methods can be implemented using different choices of D . We make use of state-of-the-art clean-label poisoning attacks, which can be generally divided into two categories: *feature collision* [36] and *gradient matching* [12]. Specifically, we employ the multi-target version of *feature collision* proposed by Aghakhani et al. [1] in our framework:

$$\begin{aligned} D(\mathcal{S}'_p, \mathcal{S}_t) &= D_{\text{FC}}(\mathcal{S}'_p, \mathcal{S}_t) \\ &= \left\| \frac{1}{|\mathcal{S}'_p|} \sum_{\mathbf{x}_p \in \mathcal{S}'_p} f(\mathcal{A}(\mathbf{x}_p)) - \frac{1}{|\mathcal{S}_t|} \sum_{\mathbf{x}_t \in \mathcal{S}_t} f(\mathbf{x}_t) \right\|_2^2, \end{aligned} \quad (5)$$

where f represents the surrogate model before the penultimate layer, known as the feature extractor. Our threat model Section 4.1 has restricted that the samples that follow \mathcal{D}_t are similar to each other. Therefore, it is reasonable to choose the *mean feature* of the subpopulation to attack and expect that the attack can generalize to the distribution.

To involve the *gradient matching* in our framework, we first need to derive the gradients of the target and poisoned

Algorithm 1: Generalizable Targeted Clean-label Poisoning Attack

Input: Clean surrogate model $F(\cdot, \theta)$, subpopulation target set \mathcal{S}_t , adversarial target class y^{adv} , clean training set $\mathcal{S} = \mathcal{S}_c \cup \mathcal{S}_p$, perturbation bound ε , optimization steps M , retraining times R

Randomly initialize perturbations $\Delta \in \mathcal{C}$;
 $\mathcal{S}'_p \leftarrow \{(x_i^p + \delta_i, y^{\text{adv}})\}_{i=1}^P$; $\triangleright \mathcal{S}'_p$ will dynamically change with Δ

for $k = 1, \dots, M$ **do**

- Compute the gradient matching loss $D_{\text{our}}(\mathcal{L}_p, \mathcal{L}_t)$ with respect to \mathcal{S}'_p and \mathcal{S}_t ; $\triangleright D_{\text{our}}$ is defined in Equation 8
- Update Δ using projected gradient descent on $D_{\text{our}}(\mathcal{L}_p, \mathcal{L}_t)$;
- Project Δ onto $\|\Delta\|_\infty \leq \varepsilon$;
- Retrain the surrogate model θ using poisoned set $\mathcal{S}' = \mathcal{S}_c \cup \mathcal{S}'_p$ every $\lfloor M/(R+1) \rfloor$ iterations except $k = M$;

end

Output: Poisoned dataset $\mathcal{S}' = \mathcal{S}_c \cup \mathcal{S}'_p$

sets, then compute some distance between the gradients:

$$\mathcal{L}_p = \mathcal{L}(F, \mathcal{A}, \theta, \mathcal{S}'_p), \quad \mathcal{L}_t = \mathcal{L}(F, \emptyset, \theta, \mathcal{S}_t),$$

where \emptyset denotes the data augmentation is disabled. Then we can formulate the *gradient matching* method:

$$D(\mathcal{S}'_p, \mathcal{S}_t) = D_{\text{GM}}(\mathcal{L}_p, \mathcal{L}_t).$$

We note that D_{GM} can have multiple choices Geiping et al. [12], such as negative cosine similarity and Euclidean distance. To be more specific, these distances are formulated as:

$$D_{\text{cos}}(\mathcal{L}_p, \mathcal{L}_t) = 1 - \cos(\nabla_{\theta} \mathcal{L}_p, \nabla_{\theta} \mathcal{L}_t), \quad (6)$$

$$D_{\text{ED}}(\mathcal{L}_p, \mathcal{L}_t) = \|\nabla_{\theta} \mathcal{L}_p - \nabla_{\theta} \mathcal{L}_t\|_2^2. \quad (7)$$

Our Matching Loss. Although D_{ED} performs worse than D_{cos} in [12] and the benchmark experiments in Section 6, it performs better in our threat model (see results in Section 5.1). Therefore, we expect that combining the cosine similarity and Euclidean distance losses can yield a better gradient alignment between the poisoning samples and the target samples, resulting in our new gradient-matching loss:

$$D_{\text{our}}(\mathcal{L}_p, \mathcal{L}_t) = D_{\text{ED}}(\mathcal{L}_p, \mathcal{L}_t) \cdot D_{\text{cos}}(\mathcal{L}_p, \mathcal{L}_t). \quad (8)$$

The poisoning perturbation will be optimized based on the above gradient matching loss and a projected gradient descent (PGD) scheme [27]. We further discuss these gradient matching methods in Section 6, where our benchmark experiment confirms the superiority of D_{our} under the conventional targeted clean-label poisoning attack settings.

5. Experiments

We empirically validate the proposed attack to various target choices in both *white-box* and *black-box* settings in this section. Our proposed attack framework mainly focuses on the training-from-scratch scenario, which is challenging to

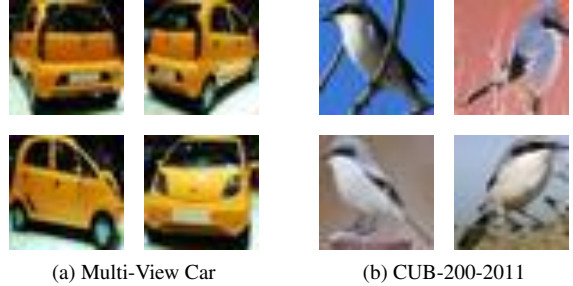


Figure 2: Illustrations of different target samples used in our experiments: (a) a Multi-View Car target with different viewpoints, and (b) a CUB-200-2011 target from the same bird species but with varying appearances.

the adversary because the model’s variation during the training process makes it hard to construct effective adversarial poisons. The Multi-View Car dataset [30] is utilized to examine the generalizability of the attack across different viewpoints of the target object. The CUB-200-2011 dataset [40] is employed to evaluate the attack’s effectiveness on various individuals of the same species. Figure 2 visualizes some examples from these datasets.

5.1. Evaluations on Cars and Birds

Datasets. To evaluate the attack’s performance in different target settings, we derive the target from the Multi-View Car dataset [30] and the CUB-200-2011 dataset [40].

The Multi-View Car dataset contains 20 different cars, each with more than 100 images taken from various viewpoints. We regard a specific car as the target, and this experiment aims to demonstrate the targeted poisoning attack’s cross-viewpoint generalizability. This subpopulation setting follows [1] where they referred to this setting as poisoning to multiple unknown images. Although the target’s variation in such a setting is moderate, this setting can be

Table 1: *White-box* evaluations of poisoning to different targets. “w/o” denotes training the model without any data poisoning.

Dataset	Victim Model	Overall Accuracy (%)					Attack Success Rate (%)				
		w/o	FC	Cosine	ED	Ours	w/o	FC	Cosine	ED	Ours
Multi-View Car	ConvNet	85.21	84.92	85.09	84.62	84.91	0.00	47.75	30.38	75.43	76.48
	VGG11	88.89	88.63	88.89	88.66	88.80	0.67	15.40	75.15	77.30	84.44
	ResNet-18	92.15	91.84	91.99	91.94	91.99	1.11	28.00	82.40	87.29	90.13
	MobileNet-V2	88.21	87.91	88.10	87.74	87.93	0.64	45.93	67.03	68.09	81.87
CUB-200-2011	ConvNet	85.21	84.82	85.08	84.30	84.55	1.17	23.83	14.47	48.46	50.70
	VGG11	88.89	88.55	88.79	88.24	88.43	0.33	19.14	47.45	58.27	61.72
	ResNet-18	92.15	91.58	91.91	91.61	91.75	0.67	15.20	59.94	65.86	71.24
	MobileNet-V2	88.21	87.69	88.04	87.41	87.56	0.17	38.24	37.47	64.20	65.26

Table 2: Attack success rate (%) for *black-box* evaluations. The adversary constructs poisoned samples via a VGG11 model, and we validate them in the corresponding models.

Victim	FC	Cosine	ED	Ours
ResNet-18	9.61	61.13	69.67	80.17
MobileNet-V2	10.40	41.46	74.20	74.42
LeViT-384	3.35	51.34	59.45	61.09
Average	7.79	51.31	67.77	71.89

regarded as a realistic threat in some scenarios, such as autonomous driving. The CUB-200-2011 dataset contains 200 bird species, which provides a looser variation setting that the target is a specific bird species. Since the model trained on the CIFAR-10 cannot accurately classify all bird species in the CUB-200-2011, we constructed our target by selecting the top 20 classes with the highest classification accuracy. This experiment aims to demonstrate the generalizable targeted poisoning attack’s cross-object generalizability.

Settings. The victim model is trained on the CIFAR-10 training dataset under the training-from-scratch scenario. To align with the image size in CIFAR-10, we resize all the images from The Multi-View Car and CUB-200-2011 into 32×32 RGB images. If not mentioned specifically, the experiment is conducted on the Multi-View Car dataset with a ResNet-18 model. The adversary contaminates 1% CIFAR-10 with the following hyperparameters used in Algorithm 1: $\epsilon = 16$, $M = 250$, and $R = 4$. Both the adversary and the victim enable the differentiable data augmentation in the model training process [12]. We present the models’ training details in Appendix D.

Main results. Table 1 demonstrates the generalizable poisoning attack’s success rate in various model architectures. Each data is obtained from 10 experiments with a randomly selected target and a random model initialization. As a re-

Table 3: Clean accuracy (%) and attack success rate (%) against different defenses. Here, the kernel size for Gaussian is set as 3 with a standard deviation of 0.1. The JPEG’s quality factor is 10, and the BDR’s bit depth is 2.

Defense	w/o	Gaussian	JPEG	BDR
Clean Acc.	91.99	91.92	83.60	89.28
ASR	90.13	90.02	0.07	2.48

sult, our generalizable targeted poisoning attack framework can generalize from the known samples to the unknown samples, and our proposed adversarial loss has shown superiority in various settings. By making a comparison between Multi-View Car and CUB-200-2011, the looser variation setting makes the target more robust to the attack. We also present the collateral damage to the overall accuracy of the validation set. It is reasonable that a stronger attack leads to more significant collateral damage. Compared to directly optimizing Euclidean distance, our attack achieved a higher success rate while causing less collateral damage.

Cross-model transferability. We validate our proposed attack’s effectiveness in the *black-box* scenario where the adversary creates the poison samples via a surrogate model, and we evaluate them in another model with a different architecture. Here we adopt VGG11 as the surrogate model due to its superiority in transferability. See Appendix A for detailed comparisons. Table 2 displays the experiment results, where our proposed method outperforms others. Although VGG11 is a model based on convolutional neural networks, the adversarial poisoned samples constructed on it can successfully transfer into the LeViT-384 [14] model, which involves attention layers.

Data augmentation. The targeted poisoning attack is sensitive to data augmentation. The default option for the adversary is enabling the data augmentation, while the victim

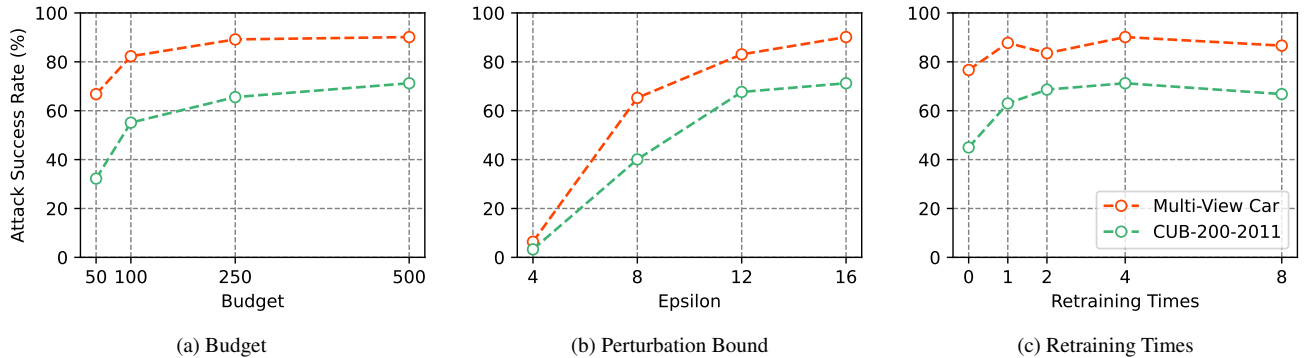


Figure 3: Ablation results on attack budget, perturbation bound, and retraining times.

Table 4: Attack success rate (%) of the experiments on data augmentations. Here, *Victim Aug.* denotes whether the victim enables data augmentation during training, and *Adv. Aug.* denotes whether the adversary enables data augmentation during the adversarial learning process.

Victim Aug.	Adv. Aug.	FC	Cosine	ED	Ours
✓	✓	28.00	82.40	87.29	90.13
X	✓	7.39	12.14	29.13	33.57
X	X	11.29	39.26	81.17	79.42

may not enable it. We demonstrate whether the victim enables data augmentation in Table 4, where the attack’s success rate has dropped significantly when the data augmentation settings of the victim and adversary are not aligned. This result is consistent with the observations in [12].

Defenses. Many defense strategies are proposed to alleviate the threat of clean-label indiscriminate poisoning attacks [31]. Here, we adapt three simple image process defensive methods discussed in Liu et al. [26]: Gaussian blur, JPEG compression, and bit depth reduction (BDR). We expect these simple processes, which filter the adversarial perturbation, to defeat the targeted poisoning attacks effectively. Table 3 reports the different defense strategies’ performances, where there is a tradeoff between the defense performance and the model’s classification accuracy. The JPEG and BDR have invalidated the poison samples, and BDR has a smaller impact on model performance.

5.2. Ablation Studies

Attack budget. According to [5], when a practical adversary wants to inject poison samples into the training set, they need to invest the cost to spread the data on the Internet. Injecting more poison samples means the adversary will incur a higher cost. Therefore, an attack is more threatening if the adversary achieves the object at a lower cost.

Here, we use the attack budget to denote the poison samples in the training set. Figure 3a reports the relationship between the attack budget and the attack’s success rate. A higher attack budget brings a higher attack success rate, and our attack can achieve acceptable performance even if the attack budget is 0.2% of the training set size. The looser target setting (CUB-200-2011) is more sensitive to the attack budget.

Perturbation bound. To satisfy the clean-label setting, a L_∞ -norm ϵ -bound is used to limit the perturbations. However, a smaller ϵ choice will bring a more subtle alteration to the poison samples, making the attack more stealthy. This ablation study is to reveal how small a ϵ the attack can succeed with. Figure 3b reports how different ϵ impacts the attack success rate, where the ϵ influences it more significantly than the attack budget. The attack achieves an acceptable performance only the $\epsilon \geq 8$.

Retraining. To validate whether the retraining process [38] is effective on our attack framework, we conduct the ablation study with different retraining times. The results in Figure 3c show the more retraining times, the better performance the attack can achieve, consistent with the result of Souri et al. [38]. However, when there are too many retraining times, the attack’s performance will not significantly improve. The number of retraining times is linearly related to the computational cost of adversarial learning, so excessive retraining times are expensive for the adversary.

6. A Second Look at Gradient Matching

The great success of Witches’ Brew [12] demonstrates the immense potential of the gradient matching technique in poisoning attacks. Gradient matching can be implemented in several ways, as we have demonstrated in Section 4.2. We can align the gradients’ direction by optimizing D_{\cos} and minimize the gradients’ Euclidean distance by optimizing D_{ED} . Apparently, for the small or thin models, when

Table 5: Attack success rate (%) on the benchmark presented by Schwarzschild et al. [35]. We demonstrate average poisoning accuracy in CIFAR-10, contaminating 1% samples with $\varepsilon = 8$. The previous works’ performances come from [12, 35]. Poisoned samples are created with a ResNet-18 model. K denotes the model ensemble’s size, where an ensemble contains several models with different initializations.

Attack	ResNet-18	MobileNet-V2	VGG11	Average
Poison Frogs [36]	0.00	1.00	3.00	1.33
Convex Polytopes [47]	0.00	1.00	1.00	0.67
Bullseye [1]	3.00	3.00	1.00	2.33
Witches’ Brew [12] ($K = 1$)	45.00	36.00	8.00	29.67
Witches’ Brew ($K = 4$)	55.00	37.00	7.00	33.00
Euclidean Distance ($K = 1$)	19.00	7.00	30.00	18.67
Ours ($K = 1$)	52.00	42.00	20.00	38.00
Ours ($K = 4$)	61.00	57.00	19.00	45.67
Ours ($K = 1$, Retrain)	38.00	27.00	6.00	23.67

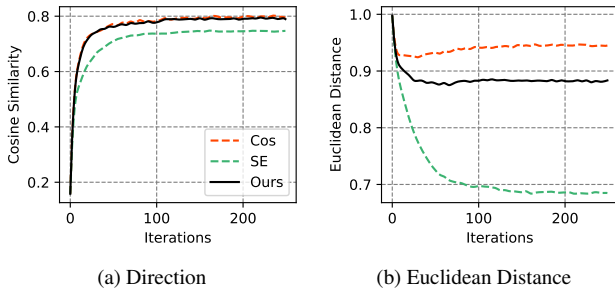


Figure 4: Direction and Euclidean distance in the adversarial optimization. The adversary performs a conventional targeted poisoning attack in ResNet-18 with data augmentation, contaminating 1% images of CIFAR-10 with $\varepsilon = 16$.

aligning the magnitude of the gradient’s difference, due to the small scale of the optimization problem, it is possible to obtain the perturbations that make $\|\nabla_{\theta}\mathcal{L}_p - \nabla_{\theta}\mathcal{L}_t\|_2^2 \approx 0$. In other words, $\mathcal{L}_p \approx \mathcal{L}_t$ denotes the direction that can be simultaneously aligned. Therefore, using D_{ED} for alignment becomes a better choice as the model becomes smaller.

Regarding a larger model, the conclusion is not so trivial. We visualize the influence of different matching strategies’ on the gradient’s cosine similarity and Euclidean distance in Figure 4. Although optimizing D_{ED} can induce a smaller Euclidean distance between gradients, it cannot align the direction as well as D_{cos} . Optimizing D_{cos} thoroughly ignores the influence of the Euclidean distance. Our proposed adversarial loss D_{our} combines the cosine similarity and Euclidean distance, which can align the gradient’s direction as much as D_{cos} and simultaneously minimize the Euclidean distance. We exploit the existing benchmark in data poisoning attacks to evaluate this adversarial loss’s performance. Table 5 reports the benchmark results,

which denotes that our method outperforms existing methods. Notably, our adversarial loss shows better transferability than previous works. Adversarial samples obtained via the ResNet-18 model can also achieve considerable attack results on the MobileNet-V2 and VGG11 models, which indicates that our method has improved the performance in the *black-box* scenario. Our experiments also validate that the retraining strategy only works on the subpopulation-targeted poisoning attack while it does not apply to the conventional targeted poisoning attack.

7. Conclusion

We introduced the problem of generalizable targeted clean-label poisoning attacks. Compared with the prior work on targeted poisoning attacks, the adversary’s objective considers the challenging scenario where the real targets are not known to the adversary during optimization. More concretely, we proposed a simple yet effective method to improve targeted attacks in such a realistic scenario. In particular, we explored diverse target variations, such as an object with varied viewpoints and an animal species with varied appearances. Our experiments indicate that the clean-label data poisoning can be generalized to the unknown samples under the training-from-scratch scenario. We also tested the defense strategies for preventing such attacks.

References

- [1] Hojjat Aghakhani, Dongyu Meng, Yu-Xiang Wang, Christopher Kruegel, and Giovanni Vigna. Bullseye polytope: A scalable clean-label poisoning attack with improved transferability. In *2021 IEEE European symposium on security and privacy (EuroS&P)*, pages 159–178. IEEE, 2021. 1, 2, 3, 4, 5, 8
- [2] Mauro Barni, Kassem Kallas, and Benedetta Tondi. A new backdoor attack in cnns by training set corruption without label poisoning. In *2019 IEEE International Conference on Image Processing (ICIP)*, pages 101–105. IEEE, 2019. 3
- [3] Battista Biggio, Blaine Nelson, and Pavel Laskov. Support vector machines under adversarial label noise. In *Asian conference on machine learning*, pages 97–112. PMLR, 2011. 1, 2
- [4] Battista Biggio, Blaine Nelson, and Pavel Laskov. Poisoning attacks against support vector machines. *arXiv preprint arXiv:1206.6389*, 2012. 1, 2
- [5] Nicholas Carlini, Matthew Jagielski, Christopher A Choquette-Choo, Daniel Paleka, Will Pearce, Hyrum Anderson, Andreas Terzis, Kurt Thomas, and Florian Tramèr. Poisoning web-scale training datasets is practical. In *2024 IEEE Symposium on Security and Privacy (SP)*, pages 407–425. IEEE, 2024. 1, 7
- [6] Soravit Changpinyo, Piyush Sharma, Nan Ding, and Radu Soricut. Conceptual 12m: Pushing web-scale image-text pre-training to recognize long-tail visual concepts. In *Proceedings of the IEEE/CVF conference on computer vision and pattern recognition*, pages 3558–3568, 2021. 1
- [7] Antonio Emanuele Cinà, Kathrin Grosse, Ambra Demontis, Sebastiano Vascon, Werner Zellinger, Bernhard A Moser, Alina Oprea, Battista Biggio, Marcello Pelillo, and Fabio Roli. Wild patterns reloaded: A survey of machine learning security against training data poisoning. *ACM Computing Surveys*, 55(13s):1–39, 2023. 1, 2, 3
- [8] Khoa Doan, Yingjie Lao, Weijie Zhao, and Ping Li. Lira: Learnable, imperceptible and robust backdoor attacks. In *Proceedings of the IEEE/CVF international conference on computer vision*, pages 11966–11976, 2021. 3
- [9] Ji Feng, Qi-Zhi Cai, and Zhi-Hua Zhou. Learning to confuse: Generating training time adversarial data with auto-encoder. In *Advances in Neural Information Processing Systems*, 2019. 1, 2
- [10] Liam Fowl, Micah Goldblum, Ping-yeh Chiang, Jonas Geiping, Wojciech Czaja, and Tom Goldstein. Adversarial examples make strong poisons. *Advances in Neural Information Processing Systems*, 34:30339–30351, 2021. 1, 2
- [11] Samir Yitzhak Gadre, Gabriel Ilharco, Alex Fang, Jonathan Hayase, Georgios Smyrnis, Thao Nguyen, Ryan Marten, Mitchell Wortsman, Dhruva Ghosh, Jieyu Zhang, et al. Datacomp: In search of the next generation of multimodal datasets. *Advances in Neural Information Processing Systems*, 36, 2024. 1
- [12] Jonas Geiping, Liam H Fowl, W. Ronny Huang, Wojciech Czaja, Gavin Taylor, Michael Moeller, and Tom Goldstein. Witches’ brew: Industrial scale data poisoning via gradient matching. In *International Conference on Learning Representations*, 2021. 1, 2, 3, 4, 5, 6, 7, 8, 11
- [13] Micah Goldblum, Dimitris Tsipras, Chulin Xie, Xinyun Chen, Avi Schwarzschild, Dawn Song, Aleksander Madry, Bo Li, and Tom Goldstein. Dataset security for machine learning: Data poisoning, backdoor attacks, and defenses. *IEEE Transactions on Pattern Analysis and Machine Intelligence*, 45(2):1563–1580, 2023. 2
- [14] Benjamin Graham, Alaaeldin El-Nouby, Hugo Touvron, Pierre Stock, Armand Joulin, Hervé Jégou, and Matthijs Douze. Levit: a vision transformer in convnet’s clothing for faster inference. In *Proceedings of the IEEE/CVF international conference on computer vision*, pages 12259–12269, 2021. 6
- [15] Tianyu Gu, Brendan Dolan-Gavitt, and Siddharth Garg. Badnets: Identifying vulnerabilities in the machine learning model supply chain. *arXiv preprint arXiv:1708.06733*, 2017. 1, 4
- [16] Tianyu Gu, Kang Liu, Brendan Dolan-Gavitt, and Siddharth Garg. Badnets: Evaluating backdooring attacks on deep neural networks. *IEEE Access*, 7:47230–47244, 2019. 3
- [17] Isha Gupta, Hidde Lycklama, Emanuel Opel, Evan Rose, and Anwar Hithnawi. Fragile giants: Understanding the susceptibility of models to subpopulation attacks, 2024. 2, 3, 4
- [18] Hanxun Huang, Xingjun Ma, Sarah Monazam Erfani, James Bailey, and Yisen Wang. Unlearnable examples: Making personal data unexploitable. *arXiv preprint arXiv:2101.04898*, 2021. 1, 2
- [19] W Ronny Huang, Jonas Geiping, Liam Fowl, Gavin Taylor, and Tom Goldstein. Metapoisson: Practical general-purpose clean-label data poisoning. *Advances in Neural Information Processing Systems*, 33:12080–12091, 2020. 1, 2, 4
- [20] Matthew Jagielski, Giorgio Severi, Niklas Pousette Harger, and Alina Oprea. Subpopulation data poisoning attacks. In *Proceedings of the 2021 ACM SIGSAC Conference on Computer and Communications Security*, pages 3104–3122, 2021. 2, 3, 4, 11
- [21] Pang Wei Koh and Percy Liang. Understanding black-box predictions via influence functions. In *International conference on machine learning*, pages 1885–1894. PMLR, 2017. 1, 2
- [22] Ram Shankar Siva Kumar, Magnus Nyström, John Lambert, Andrew Marshall, Mario Goertzel, Andi Comissioneru, Matt Swann, and Sharon Xia. Adversarial machine learning-industry perspectives. In *2020 IEEE security and privacy workshops (SPW)*, pages 69–75. IEEE, 2020. 1
- [23] Shaofeng Li, Minhui Xue, Benjamin Zi Hao Zhao, Haojin Zhu, and Xinpeng Zhang. Invisible backdoor attacks on deep neural networks via steganography and regularization. *IEEE Transactions on Dependable and Secure Computing*, 18(5):2088–2105, 2020. 3
- [24] Yuezun Li, Yiming Li, Baoyuan Wu, Longkang Li, Ran He, and Siwei Lyu. Invisible backdoor attack with sample-specific triggers. In *Proceedings of the IEEE/CVF international conference on computer vision*, pages 16463–16472, 2021. 1, 3
- [25] Yunfei Liu, Xingjun Ma, James Bailey, and Feng Lu. Reflection backdoor: A natural backdoor attack on deep neural

- networks. In *Computer Vision—ECCV 2020: 16th European Conference, Glasgow, UK, August 23–28, 2020, Proceedings, Part X 16*, pages 182–199. Springer, 2020. 3
- [26] Zhuoran Liu, Zhengyu Zhao, and Martha Larson. Image shortcut squeezing: Countering perturbative availability poisons with compression. In *International conference on machine learning*, pages 22473–22487. PMLR, 2023. 7
- [27] Aleksander Madry. Towards deep learning models resistant to adversarial attacks. *arXiv preprint arXiv:1706.06083*, 2017. 5
- [28] Luis Muñoz-González, Battista Biggio, Ambra Demontis, Andrea Paudice, Vasin Wongrassamee, Emil C Lupu, and Fabio Roli. Towards poisoning of deep learning algorithms with back-gradient optimization. In *Proceedings of the 10th ACM workshop on artificial intelligence and security*, pages 27–38, 2017. 1, 2, 4
- [29] Tuan Anh Nguyen and Anh Tuan Tran. Wanet - imperceptible warping-based backdoor attack. In *International Conference on Learning Representations*, 2021. 3
- [30] Mustafa Ozuysal, Vincent Lepetit, and Pascal Fua. Pose estimation for category specific multiview object localization. In *2009 IEEE Conference on Computer Vision and Pattern Recognition*, pages 778–785. IEEE, 2009. 5
- [31] Tianrui Qin, Xitong Gao, Juanjuan Zhao, Kejiang Ye, and Cheng-Zhong Xu. Apbench: A unified benchmark for availability poisoning attacks and defenses. *arXiv preprint arXiv:2308.03258*, 2023. 7
- [32] Evan Rose, Fnu Suya, and David Evans. Understanding variation in subpopulation susceptibility to poisoning attacks. *arXiv preprint arXiv:2311.11544*, 2023. 3, 4
- [33] Aniruddha Saha, Akshayvarun Subramanya, and Hamed Pirsiavash. Hidden trigger backdoor attacks, 2019. 1, 3
- [34] Christoph Schuhmann, Romain Beaumont, Richard Vencu, Cade Gordon, Ross Wightman, Mehdi Cherti, Theo Coombes, Aarush Katta, Clayton Mullis, Mitchell Wortsman, et al. Laion-5b: An open large-scale dataset for training next generation image-text models. *Advances in Neural Information Processing Systems*, 35:25278–25294, 2022. 1
- [35] Avi Schwarzschild, Micah Goldblum, Arjun Gupta, John P Dickerson, and Tom Goldstein. Just how toxic is data poisoning? a unified benchmark for backdoor and data poisoning attacks. In *International Conference on Machine Learning*, pages 9389–9398. PMLR, 2021. 8, 11
- [36] Ali Shafahi, W Ronny Huang, Mahyar Najibi, Octavian Suciu, Christoph Studer, Tudor Dumitras, and Tom Goldstein. Poison frogs! targeted clean-label poisoning attacks on neural networks. *Advances in neural information processing systems*, 31, 2018. 1, 2, 3, 4, 8
- [37] Piyush Sharma, Nan Ding, Sebastian Goodman, and Radu Soricut. Conceptual captions: A cleaned, hypernymed, image alt-text dataset for automatic image captioning. In *Proceedings of the 56th Annual Meeting of the Association for Computational Linguistics (Volume 1: Long Papers)*, pages 2556–2565, 2018. 1
- [38] Hossein Souri, Liam Fowl, Rama Chellappa, Micah Goldblum, and Tom Goldstein. Sleeper agent: Scalable hidden trigger backdoors for neural networks trained from scratch. *Advances in Neural Information Processing Systems*, 35: 19165–19178, 2022. 1, 3, 4, 7
- [39] Jacob Steinhardt, Pang Wei W Koh, and Percy S Liang. Certified defenses for data poisoning attacks. *Advances in neural information processing systems*, 30, 2017. 3
- [40] Catherine Wah, Steve Branson, Peter Welinder, Pietro Perona, and Serge Belongie. The caltech-ucsd birds-200-2011 dataset, 2011. 5
- [41] Emily Wenger, Josephine Passananti, Arjun Nitin Bhagoji, Yuanshun Yao, Haitao Zheng, and Ben Y Zhao. Backdoor attacks against deep learning systems in the physical world. In *Proceedings of the IEEE/CVF conference on computer vision and pattern recognition*, pages 6206–6215, 2021. 3
- [42] Emily Wenger, Roma Bhattacharjee, Arjun Nitin Bhagoji, Josephine Passananti, Emilio Andere, Haitao Zheng, and Ben Y Zhao. Natural backdoor datasets. *arXiv preprint arXiv:2206.10673*, 2022. 3
- [43] Han Xiao, Huang Xiao, and Claudia Eckert. Adversarial label flips attack on support vector machines. In *ECAI 2012*, pages 870–875. IOS Press, 2012. 1
- [44] Huang Xiao, Battista Biggio, Gavin Brown, Giorgio Fumera, Claudia Eckert, and Fabio Roli. Is feature selection secure against training data poisoning? In *international conference on machine learning*, pages 1689–1698. PMLR, 2015.
- [45] Huang Xiao, Battista Biggio, Blaine Nelson, Han Xiao, Claudia Eckert, and Fabio Roli. Support vector machines under adversarial label contamination. *Neurocomputing*, 160: 53–62, 2015. 1
- [46] Yuanshun Yao, Huiying Li, Haitao Zheng, and Ben Y Zhao. Latent backdoor attacks on deep neural networks. In *Proceedings of the 2019 ACM SIGSAC conference on computer and communications security*, pages 2041–2055, 2019. 1
- [47] Chen Zhu, W Ronny Huang, Hengduo Li, Gavin Taylor, Christoph Studer, and Tom Goldstein. Transferable clean-label poisoning attacks on deep neural nets. In *International conference on machine learning*, pages 7614–7623. PMLR, 2019. 2, 8

Table 6: Attack transferability (%) under the Multi-View Car settings. Here, attacks are transferred from the models in rows to those in columns.

Model	RN-18	MobileNet	VGG11	LeViT	Avg.
RN-18	90.13	40.78	17.18	10.10	39.55
MobileNet	60.68	81.87	30.60	15.70	47.21
VGG11	80.17	74.42	84.44	61.09	75.03
LeViT	32.89	14.03	57.32	81.97	46.55

Table 7: Attack success rate (%) for subpopulation poisoning attack evaluations.

Victim	FC	Cosine	ED	Ours
ResNet-18	9.91	12.76	21.38	29.34

A. Attack Transferability across Models

Table 6 reports the transfer attack success rate with different surrogate models. As can be seen, the ResNet-18, which is commonly adopted Schwarzschild et al. [35], indeed achieves the worst transferability in our threat model. In contrast, the VGG, which does not contain residual modules, shows the best results. Furthermore, the poison samples can transfer from CNNs to ViTs. Our additional results also confirm that the transferability depends on the architectural similarity between the surrogate and target models. Specifically, transferring from VGG11 to LeViT, which contains four convolutional layers, yields better transferability than Swin, which contains only one convolutional layer (61.09% vs. 41.03%).

B. Subpopulation Evaluations on CIFAR-10

We consider a more challenging generalization setting to explore the limit of our proposed attacks further. In this setting, we consider the generalization across different feature clusters, following the conventional subpopulation attack problem [20].

In particular, we leverage the ClusterMatch [20] to divide each class of CIFAR-10 into 50 clusters as the subpopulations. The adversarial poison samples are generated by the target samples in the training set, and we validate the attack’s performance on the target samples in the validation set. Table 7 reports the results. As expected, all attacks become substantially worse compared to those on Table 1. However, our method remains the best.

C. Potential Randomness in Experiments

We have followed existing work [12] to avoid the impact of randomness in our experiments. Specifically, in each experiment, we tested 10 combinations of targets and intended

classes chosen randomly. For Section 5.1, since the model’s randomization will influence the attack performance of the poisoned samples, for each combination, we train the victim model on the poisoned dataset 8 times to perform the evaluation.

D. Model and Training Hyperparameters

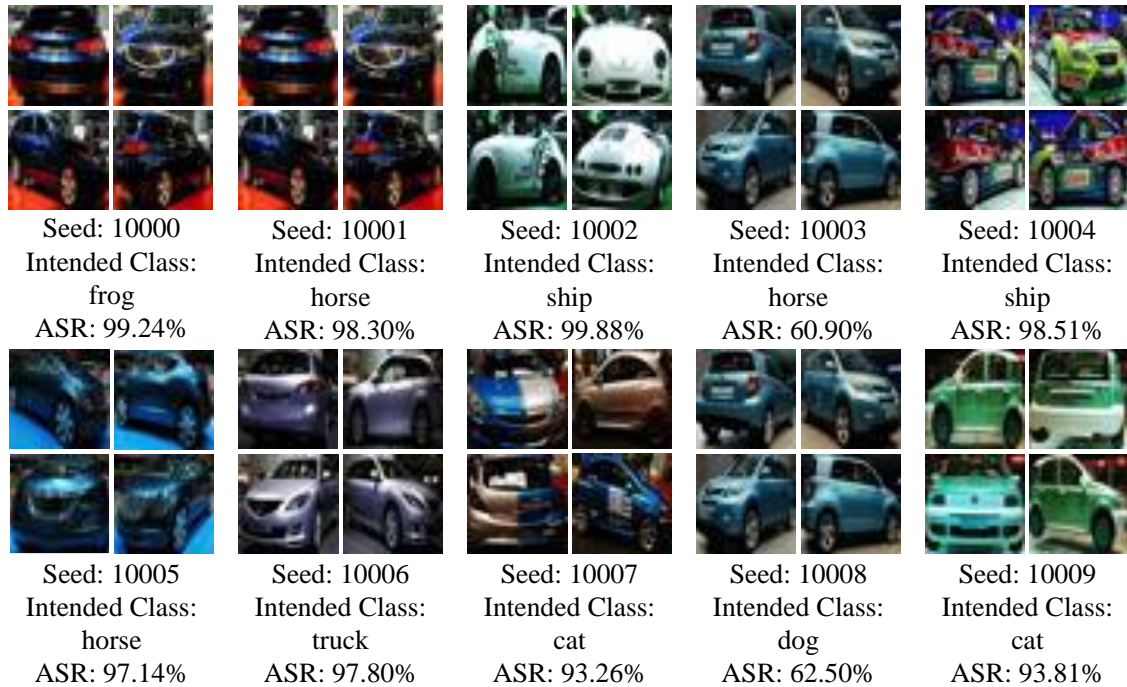
For the experiments on Section 5.1, we consider 5 neural network models: ConvNet, ResNet-18, VGG-11, MobileNet V2, and LeViT-384. The ConvNet we considered contains 5 convolutional layers with a following linear layer. Each convolutional layer is followed by a ReLU activation, and for the last two convolutional layers, each layer is followed by a max pooling layer with size 3. The output widths of each layer are 64, 128, 128, 256, 256, 2304. The ResNet-18 setting is followed by Witches’ Brew [12], where they modify the first convolutional layer with a kernel size of 3. VGG-11, MobileNet V2, and LeViT-384 are with their standard configurations.

We set the learning rate to 0.1 for ResNet-18 and 0.01 for the others. The batch size is 512 for LeViT-384 and 128 for the others. We train the ConvNet, ResNet-18, VGG-11, and MobileNet V2 for 40 epochs and schedule the learning rate drops at epochs 14, 24, and 35 by a factor of 0.1. Since the ViTs need more epochs to converge, the total number of training epochs of LeViT-384 is set to 100. We adjust the learning rate dropping at epochs 37, 62, and 87 by a factor of 0.1. We apply the data augmentation that horizontally flips the image with a probability of 0.5 and randomly crops a size 32×32 with a zero-padding of 4.

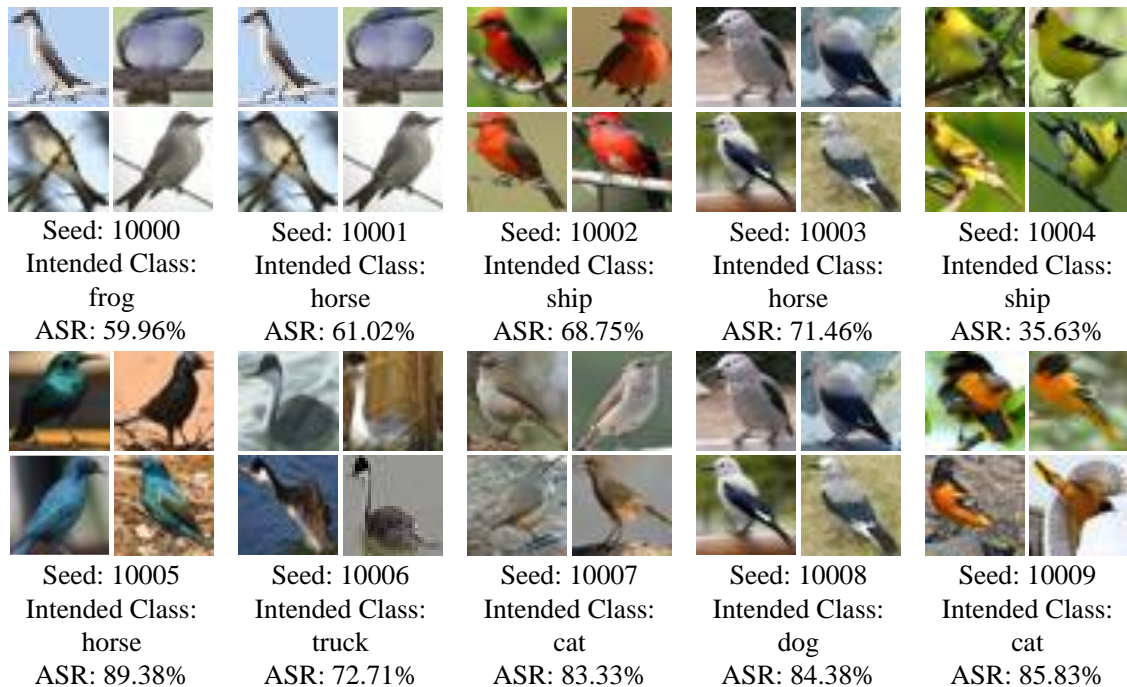
The Swin Transformer we discussed in Appendix A is a modified Swin V2 Tiny model that reduces the patch size from 4 to 2 and the window size from 8 to 4. We train this model with a learning rate of 0.01 for 100 epochs and drop the learning rate at epochs 50, 75, and 90 by a factor of 0.1.

E. Visualization of Target Samples

This section presents the target sample selection of each random seed. We have applied random seeds from 10000 to 10009 in our experiments. Figure 5 displays the targets in Section 5.1, where the target samples are derived based on the provided annotations.



(a) Visualizations of car targets.



(b) Visualizations of bird targets.

Figure 5: Visualizations of different seeds with the corresponding targets and intended classes. Here, ASR denotes the attack success rate of our proposed method, and Intended Class denotes the class that the adversary wants to mislead the target into.